NUCLEAR THEORY, Vol. 37 (2018)
eds. M. Gaidarov, N. Minkov, Heron Press, Sofia

Gogny Forces in the Astrophysical Context

X. Viñas[1], **C. Gonzalez-Boquera**[1], **M. Centelles**[1], **L.M. Robledo**[2,3], **C. Mondal**[1]

[1]Departament de Física Quàntica i Astrofísica and Institut de Ciències del Cosmos (ICCUB), Facultat de Física, Universitat de Barcelona, Martí i Franquès 1, E-08028 Barcelona, Spain

[2]Departamento de Física Teórica, Universidad Autónoma de Madrid, E-28049 Madrid, Spain

[3]Center for Computational Simulation, Universidad Politécnica de Madrid, Campus de Montegancedo, Boadilla del Monte, 28660-Madrid, Spain

Abstract. The most successful Gogny interactions of the D1 family, namely D1S, D1N and D1M, suffer the common problem of a too soft neutron matter equation of state at high density, which prevents them from predicting a maximal mass of neutron stars of two solar masses, as required by recent astronomical observations. To cure this deficiency, we have proposed recently a reparametrization of the D1M force by fine tuning the slope of the symmetry energy in such a way that it preserves the ground-state properties of D1M in finite nuclei and also describes successfully the global properties of neutron stars, in particular its maximal mass, in consonance with the observational data. In this contribution we revisit this reparametrization by discussing two modified Gogny forces, dubbed D1M* and D1M**.

1 Introduction

The Gogny forces were established by D. Gogny more than thirty years ago in order to describe simultaneously the mean field and the pairing field with the same effective interaction [1]. These forces are specially well adapted to study ground-state properties of spherical and deformed nuclei through the Hartree-Fock-Bogoliubov (HFB) formalism in configuration space using harmonic oscillator (HO) basis. Large-scale calculations of this type [2] have been performed using the D1S parametrization of the Gogny force [3], which provide masses and radii as well as pairing and deformation properties of finite nuclei in good agreement with the experimental data. However, it was found that there is an energy drift in neutron-rich nuclei when computed with the D1S force [4]. To improve this limitation, new parametrizations of the D1 family of interactions, namely D1N [5] and D1M [6], were proposed. It should be mentioned that in order to calibrate these forces it is required that the D1N and D1M forces qualitatively reproduce the microscopic neutron matter equation of state (EOS) of Friedman

and Pandharipande [7]. The parameters of the D1N force were determined following the D1 fitting protocol [1], while the parameters of the D1M interaction were adjusted to reproduce the experimentally known masses of 2149 nuclei. This fit of the D1M force, which also takes into account the quadrupole correlation energies, predicts the experimental masses of the previously mentioned nuclei with a *rms* deviation of only 798 keV [6].

In spite of this good description of ground-state properties of finite nuclei, the extrapolation to the neutron star domain is not completely satisfactory. For example, as discussed in detail in Refs. [8–11], the successful Gogny forces of the D1 family, which nicely reproduce the ground-state properties of finite nuclei, namely D1S, D1N and D1M, are unable to reach a maximal neutron star (NS) mass of $2M_\odot$ as required by recent astronomical observations [12, 13] and only the D1M interaction predicts a NS mass above the canonical value of $1.4M_\odot$ [9–11]. This can be observed in the panel a) of Figure 1 where the mass-radius relations computed with different mean field models, including the most successful Gogny interactions, are displayed.

Some unique properties of the Gogny forces, such as its finite range and the fact that the particle-particle and the particle-hole interactions can be treated with the same force, may also have an important role in the astrophysical context. To achieve this goal, we have built two new Gogny interactions, which we call D1M* and D1M**, performing a modification of the parameters of D1M in such a way that these forces reproduce finite nuclei data in as good agreement as those obtained using D1M and, at the same time, provide a description of NS at the same level of some Skyrme forces, such as SLy4 [14], specially designed for the study of NS.

The paper is organized as follows. The first section is devoted to the fitting procedure of two new interactions namely D1M* and D1M** and to the discussion of some relevant predictions of these forces in the context of neutron stars. In the second section the ability of the D1M* interaction is analyzed by describing some selected properties of finite nuclei, comparing them with the predictions from the D1M force. Finally our conclusions are laid in the last section.

2 The D1M* and D1M** Interactions

The standard Gogny interaction of the D1 family consists of a finite range part, which is modeled by two Gaussian terms that include all the possible spin-isospin exchange terms, plus a zero-range density-dependent term. Including the spin-orbit force, which is also of contact type, the Gogny force [1] reads:

$$V(\mathbf{r}_1,\mathbf{r}_2) = \sum_{i=1,2} \left(W_i + B_i P_\sigma - H_i P_\tau - M_i P_\sigma P_\tau\right) e^{-\frac{r^2}{\mu_i^2}} + t_3(1+x_3 P^\sigma)\rho^\alpha(\mathbf{R})\delta(\mathbf{r}) + iW_{LS}(\sigma_1+\sigma_2)(\mathbf{k}'\times\delta(\mathbf{r})\mathbf{k}), \quad (1)$$

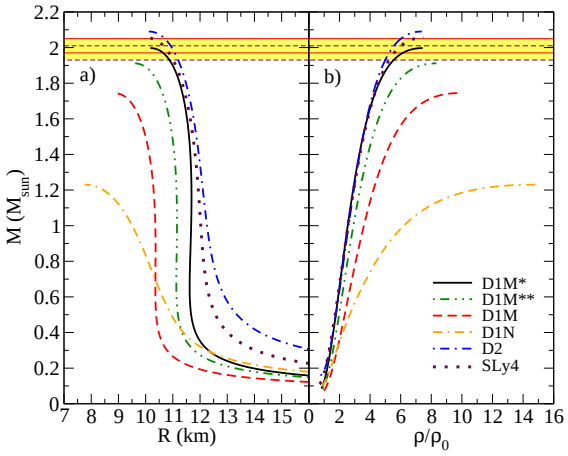

Figure 1. a) Mass-Radius relation for different Gogny forces compared with the prediction of the SLy4 Skyrme force, which is taken as a benchmark. The constraint on the observed maximum mass of neutron stars [12, 13] is depicted as the horizontal shaded region. b) Mass of neutron stars predicted by different Gogny forces and the SLy4 interaction as a function of the central density (in units of the saturation density).

where $\mathbf{r} = \mathbf{r_1} - \mathbf{r_2}$ and $\mathbf{R} = (\mathbf{r_1} + \mathbf{r_2})/2$ are the relative and the center of mass coordinates, and $\mu_1 \simeq$0.5-0.7 fm and $\mu_2 \simeq$1.2 fm are the ranges of the two Gaussian form factors, which simulate the short- and long-range components of the force, respectively.

The standard nuclear matter properties predicted by some relevant Gogny forces are displayed in Table 1. From this table we can see that the different properties of symmetric nuclear matter (SNM) *e.g.* the saturation density ρ_0, the binding energy per nucleon at saturation E_0, the incompressibility K and the effective mass m^*/m predicted by the different forces considered are rather

Table 1. Nuclear matter properties predicted by the D1M*, D1M**, D1M, D1N, D1S and D2 Gogny interactions and the SLy4 Skyrme force.

	ρ_0 (fm^{-3})	E_0 (MeV)	K (MeV)	m^*/m	$E_{\rm sym}(\rho_0)$ (MeV)	$E_{\rm sym}(0.1)$ (MeV)	L (MeV)
D1M*	0.1650	−16.06	225.4	0.746	30.25	23.82	43.18
D1M**	0.1647	−16.02	225.0	0.746	29.37	23.80	33.91
D1M	0.1647	−16.02	225.0	0.746	28.55	23.80	24.83
D1N	0.1612	−15.96	225.7	0.697	29.60	23.80	33.58
D1S	0.1633	−16.01	202.9	0.747	31.13	25.93	22.43
D2	0.1628	−16.00	209.3	0.738	31.13	24.32	44.85
SLy4	0.1596	−15.98	229.9	0.695	32.00	25.15	45.96

similar. This is because the properties of SNM at low densities are well constrained by the properties of terrestrial nuclei. However, the symmetry energy and its slope at saturation, which govern the isovector sector, differ more among the different models. We can see that some forces (the new D1M*, D1M** and D2 Gogny interactions and the SLy4 Skyrme force), which predict maximum mass of NS around $2M_\odot$ (see Figure 1), have a slope of the symmetry energy L about 45 MeV, while other forces, such as D1S, D1N and D1M, which have smaller values of the slope parameter L, are unable to reach a maximum mass of NS in excess of $2M_\odot$ as it can be seen from panel a) of Figure 1. From panel b) of Figure 1 we can also observe that those forces which are able to reach a maximal mass of $2M_\odot$ predict a central density around seven times the saturation density while forces predicting smaller maximal mass have larger central densities.

The symmetry energy is defined as $E_{\rm sym}(\rho) = \frac{1}{2}\partial^2 E_b(\rho,\delta)/\partial\delta^2|_{\delta=0}$, where $E_b(\rho,\delta)$ is the energy per particle in asymmetric nuclear matter of density $\rho = \rho_n + \rho_p$ and asymmetry $\delta = (\rho_n - \rho_p)/\rho$, ρ_n and ρ_p being the neutron and proton densities, respectively. The symmetry energy can be understood as the energy cost for converting all protons in neutrons in symmetric nuclear matter. Therefore its slope at the saturation density practically corresponds to the slope of the neutron EOS at this density and, consequently, has an important impact on the behaviour of the NS EOS at densities above saturation. The slope parameter is defined as $L = 3\rho_0 \frac{\partial E_{\rm sym}(\rho)}{\partial\rho}|_{\rho=\rho_0}$, where ρ_0 is the saturation density. This parameter L is also connected to different properties of finite nuclei, as for example the neutron skin thickness in a heavy nucleus such as ^{208}Pb (see [15,16] and references therein). The symmetry energy as a function of the density is displayed for several Gogny interactions in panel a) of Figure 2. At subsaturation densities the symmetry energy computed with all the forces shows a similar behaviour and takes a value around 30 MeV at saturation (see Table 1). In this regime the symmetry energy falls within, or lies very close, to the region constrained by the Isobaric Analog States [18], which implies that the symmetry energy predicted by these Gogny interactions is well constrained by finite nuclei data. Above saturation, the behaviour of the symmetry energy is strongly model dependent. From this figure two different patterns can be observed. On the one hand, the symmetry energy computed with the D1S, D1N and D1M interactions increases till reaching a maximum value around 30-40 MeV and then bends and decreases with increasing density until vanishing at some density where the isospin instability starts. On the other hand, the other forces, namely D1M*, D1M** and D2, predict a symmetry energy with a well defined increasing trend with growing density. This different behaviour of the symmetry energy strongly influences the EOS of the NS matter (which for simplicity we assume made of neutrons, protons and electrons in charge and β-equilibrium) as it can be seen in the panel b) of Figure 2. From this panel we observe that except the EOS obtained with the D1S interaction, the EOSs predicted by the other forces grow with increasing density. However, not all forces with an increasing EOS in NS matter are able

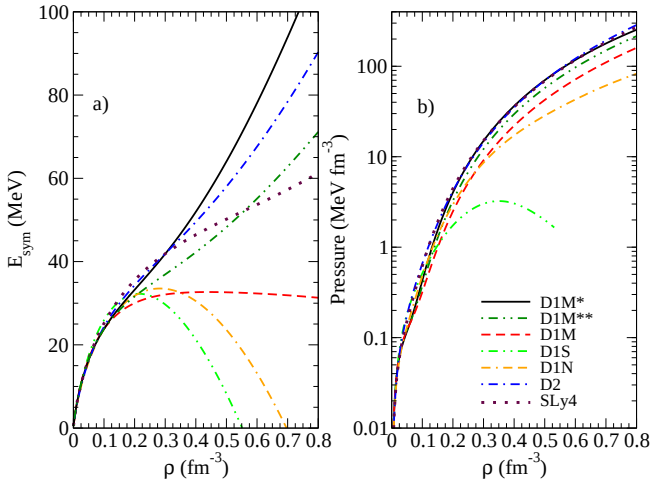

Figure 2. a) Symmetry energy computed with the D1M*, D1M**, D1M, D1N, D1S and D2 Gogny interactions and the SLy4 Skyrme force as a function of the density. b) EOS of β-stable neutron star matter as a function of the density predicted by the same forces as in panel a).

to predict a NS with maximum mass of $2M_\odot$ or above because these EOSs are too soft at high densities several times the saturation density.

In Figures 1 and 2, in addition to the standard Gogny forces D1S, D1N and D1M, we have also considered the D1M*, D1M** and D2 interactions. The D1M* force is a reparametrization of the D1M interaction introduced in Ref. [11], which leaves the description of finite nuclei with an average level of quality similar to that provided by D1M and, at the same time, is also able to predict a maximum mass of the NS of 2 $M_\odot$. The D1M** is another Gogny force built up as D1M* but predicting a maximum mass of NS of 1.91 $M_\odot$, which is close to the lower value, within the error bars, of the heaviest observed masses [12, 13]. The D2 interaction is a new Gogny force, devised by the Bruyères-le-Châtel group, which instead of the standard zero-range density-dependent term of the D1 family of Gogny forces, contains a density-dependent finite-range term [19, 20]. This force is fitted according to the D1 protocol [1] including a qualitative reproduction of the Friedman and Pandharipande EOS. This new force is free of the energy drift for exotic nuclei observed in D1S, but, as it is pointed out in [20], the description of the nuclear masses has not reached yet the quality obtained with the D1M force.

2.1 The fitting procedure

The new Gogny interaction D1M* is obtained starting from the D1M force and performing a controlled change of its parameters. This means that we only modify the finite-range spin-isospin strength coefficients keeping the ranges of the

two Gaussian form factors as well as the zero-range density dependent part of the force with the same values as in the original D1M force. In order to determine the finite-range parameters of the new Gogny interaction D1M*, we proceed in a similar way to those used in previous literatures to generate families of Skyrme interactions or RMF parametrizations, *viz.* SAMi-J [21], KED0-J [22] or TAMU-FSU [23, 24]. The basic idea to obtain these families is the following. Starting from a well calibrated and successful mean-field model, one modifies the values of some parameters, which determine the symmetry energy, around their optimal values retaining as much as possible values of the binding energies and radii of finite nuclei of the original model. Four of the eight initially free parameters of the force, namely W_i, B_i, H_i and M_i (i=1,2), are constrained by imposing that the saturation density, energy per particle, incompressibility modulus and effective mass in symmetric nuclear mater take the values corresponding to the original D1M interaction. In order to have a right behaviour of the asymmetric nuclei, we also impose that the symmetry energy in uniform matter calculated at a density of 0.1 fm^{-3} computed with D1M and D1M* to be the same. The reason of this constraint is based on the empirical law of Ref. [15], which demonstrates that the symmetry energy at some subsaturation density about 0.1 fm^{-3}, calculated with a given nuclear force, coincides with the symmetry energy of ^{208}Pb nucleus calculated with the Droplet Model [17] for the same force, which contains both, bulk and surface contributions. To preserve the pairing properties of D1M in the S=0 T=1 channel, we also impose that in the new parametrization D1M* the combination of parameters $W_i - B_i - H_i + M_i$ (i=1,2) take the same values to those in the original force D1M. With this protocol, we are able to determine seven of the eight initially free parameters of D1M* as a function of the eighth parameter, which we chose to be B_1. This free parameter is used to modify the slope of the symmetry energy at saturation and therefore, the behaviour of the neutron matter EOS above saturation, which in turn determines the maximum mass of the NS by solving the Tolman-Oppenheimer-Volkoff (TOV) equations. In this way the parameters corresponding to the finite range part of the new D1M* interaction are completely determined. We observe, however, that the description of nuclear masses provided by the D1M* force degrades slightly as compared with predictions of the original D1M interaction. To correct this deficiency, we perform in D1M* an additional small refit of the zero-range strength t_3 of about 1 MeV fm^4 to recover the same mass *rms* value to that using the D1M parametrization. The fitting protocol of the D1M** is the same only that the required maximum mass of a NS is now 1.91 $M_\odot$ instead of 2 $M_\odot$ as in the case of D1M* (see below).

The parameters of the new forces D1M* and D1M** are collected in Table 2 together with the ones of the original D1M interaction. We observe that the change of the finite range parameters, as compared with the original ones of the D1M force, is larger for the D1M* force than for the D1M** interaction because the variation in the isovector sector is more important in the former than in the latter force. Looking at the D1M family in Table 1, we see that the only nuclear

matter property that shows a relevant modification is the slope of the symmetry energy, which changes from 24.83 MeV (D1M) to 33.91 MeV (D1M**) and 43.18 MeV (D1M*). The symmetry energy at saturation also changes but in a much less extent. All the remaining nuclear matter properties of the forces of the D1M family displayed in Table 1 take the same values as a consequence of our fitting procedure. Looking at Figure 1 and keeping in mind the values of the slope of the symmetry energy of the D1M family, it can be seen that when the slope parameter of the force increases, the maximum mass of the NS predicted by the force also increases. This is, however, only a qualitative rule and exceptions may appear. For example D1N and D1M** have almost the same slope of the symmetry energy at saturation but the maximum mass predicted by the former is around 1.2 $M_\odot$ and 1.91 $M_\odot$ for the latter. This fact points out that, in spite of the same slope of the symmetry energy at saturation, the behaviour of the symmetry energy above saturation (see upper panel of Figure 2) strongly determines the EOS at high density and therefore the maximum NS mass predicted by each force.

3 Finite Nuclei Properties Described with the D1M* Force

One of the goals of parametrizing D1M* and D1M** is to reproduce nuclear structure properties of finite nuclei with the same global quality as the original D1M force. The finite nuclei calculations have been performed with the computer code HFBaxial [25] which solves the HFB equations in a HO basis using the Gogny interaction. Large-scale HFB calculations using this code and the D1M Gogny force have been done some time ago [26]. More details about the technicalities for solving the HFB equations and the minimization procedure for finding the ground-state properties have been reported in [11]. Although the calculations of finite nuclei properties with the D1M** force have not been per-

Table 2. Parameters of the D1M, D1M* and D1M** Gogny interactions, where W_i, B_i, H_i and M_i are in MeV and μ_i in fm. The coefficients $x_3 = 1$, $\alpha = 1/3$ and $W_{LS} = 115.36$ MeV fm^5 are the same in the three interactions, and t_3 has values of $t_3 = 1562.22$ MeV fm^4 for D1M and D1M** and $t_3 = 1561.22$ MeV fm^4 for D1M*

D1M	W_i	B_i	H_i	M_i	μ_i
i=1	-12797.57	14048.85	-15144.43	11963.81	0.50
i=2	490.95	-752.27	675.12	-693.57	1.00
D1M*	W_i	B_i	H_i	M_i	μ_i
i=1	-17242.0144	19604.4056	-20699.9856	16408.3344	0.50
i=2	712.2732	-982.8150	905.6650	-878.0060	1.00
D1M**	W_i	B_i	H_i	M_i	μ_i
i=1	-15019.7922	16826.6278	-17922.2078	14186.1122	0.50
i=2	583.1680	-867.5425	790.3925	-785.7880	1.00

formed as extensively as with D1M*, looking at their parameters reported in Table 2, it is expected that the predictions of D1M** will lie between the ones of D1M and D1M*. Our preliminary investigation confirms this expectation.

3.1 Binding energies and neutron and proton radii

Fine tuning of the t_3 parameter of D1M* has been performed by minimizing the *rms* deviation, σ_E, of the binding energies of 620 even-even nuclei [27]. The obtained value of 1.34 MeV is very close to the 1.36 MeV obtained for D1M under the same circumstances. This indicates a similar performance of both parametrizations in the average description of binding energies along the periodic table. The differences between the theoretical binding energies calculated with the D1M* force and the experimental values are scattered around zero and do not show any drift with increasing neutron number. The agreement between theory and experiment is good for medium and heavy nuclei and deteriorates for light nuclei, as usually happens with mean field models of different nature. This can be seen in the upper panel of Figure 5 of Ref. [11]. The differences between the binding energies computed with the D1M* and D1M are never larger than ± 2.5 MeV and show a clear shift along isotopic chains because of the different density dependence of the symmetry energy in both forces, as displayed in the lower panel of Figure 5 of Ref. [11]. The slope parameter L predicted by the D1M* force is larger than the one of D1M, as can be seen in Table 2. As a consequence [15], it is expected that for neutron-rich nuclei the radius of the neutron distribution calculated with D1M* is larger than the value obtained with D1M. On the other hand, and due to the fitting protocol to obtain the different members of the D1M family, it is also expected that the radii for the proton distribution calculated with the D1M and D1M* forces are roughly the same. The HFB calculations performed with these interactions confirm this expectation.

3.2 Potential energy surfaces

An important aspect of any nuclear interaction is the way it determines the response of the nucleus to shape deformation, in particular to the quadrupole deformation. To know if a nucleus is quadrupole deformed or not plays a crucial role in the determination of the low-energy spectrum. To study the response of the D1M* force to the quadrupole deformation, we have performed constrained HFB calculations in finite nuclei fixing the quadrupole moment Q_{20} to given values, which allow to obtain the potential energy surfaces (PES). As an example, in panel a) of Figure 3 the PES along the Er isotopic chain is displayed as a function of the deformation parameter β_2 for the original D1M interaction and for the modified D1M* force. From this figure, it can be observed that the curves corresponding to the calculations performed with the D1M and D1M* forces follow basically the same trends with a small parallel displacement of one curve with respect to the other.

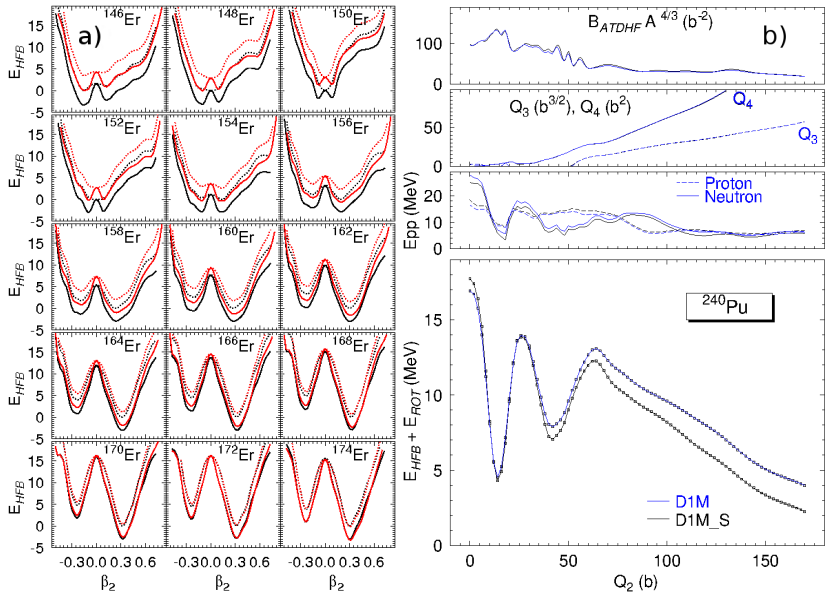

Figure 3. a) Potential energy surfaces of the Er isotopic chain computed with the D1M (red) and D1M* (black) interactions as a function of the quadrupole deformation parameter β_2. Solid and dotted curves include and do not include the rotational energy. b) Fission barrier of the nucleus ^{240}Pu as a function of the quadrupole moment Q_2 calculated with the same Gogny forces. The evolution of the mass parameter, octupole and hexadecapole moments and neutron and proton pairing energies along the fission path are also displayed in the same figure.

3.3 Fission barriers

Finally we discuss the fission barrier of the paradigmatic nucleus ^{240}Pu, which is displayed in the right bottom panel of Figure 3. We see that the inner fission barrier predicted by D1M and D1M* is the same in both models with a value B_I=9.5 MeV. This value is a little bit large compared with the "experimental" value of 6.05 MeV. However, it should be pointed out that triaxiality effects, not accounted for in the present calculation, might lower the inner barrier by 2-3 MeV. The excitation energy of the fission isomer E_{II} is 3.36 MeV computed with D1M and 2.80 MeV with D1M*. The outer fission barrier B_{II} height are 8.58 and 8.00 MeV calculated with the D1M and D1M* forces, respectively. These values clearly overestimate the empirical value, which is 5.15 MeV. In the other panels of the same figure we have also displayed as a function of the quadrupole deformation the neutron and proton pairing energies, the octupole moment (responsible for asymmetric fission) and the hexadecapole moment of the mass distributions as well as the collective inertia. All these quantities take very similar values computed with both interactions.

4 Conclusions

In this paper we have revisited some reparametrizations of the Gogny D1M force, which preserves most of its relevant properties in finite nuclei, and is still able to predict a stiffer neutron equation of state by a suitable modification of the slope of the symmetry energy. This enables one to increase the predicted maximal mass of neutron stars. We propose two different reparametrizations, namely D1M* and D1M**, which predict maximal mass of neutron stars of 2 and 1.91 solar masses, respectively, in agreement with the range of values provided by recent astronomical observations. With these modified interactions we study some basic properties of finite nuclei, such as binding energies, neutron and proton radii, response to quadrupole deformation and fission barriers. We find that both, D1M* and D1M**, perform as well as D1M in all the concerned properties of finite nuclei. We have also verified that the description of neutron star properties by these new forces are very similar to those obtained with the Skyrme SLy4 interaction, which is designed specially for working in the astrophysical scenario. To summarize, one can conclude that the D1M* and D1M** forces are a good alternative to describe simultaneously finite nuclei and neutron stars providing results in harmony with the experimental and observational data.

5 Acknowledgments

The work of L.M.R. was supported by Spanish Ministry of Economy and Competitiveness (MINECO) Grants No FPA2015-65929-P and FIS2015-63770-P. C.G., M.C., X.V. and C.M. were partially supported by Grant FIS2017-87534-P from MINECO and FEDER, and Project MDM-2014-0369 of ICCUB (Unidad de Excelencia María de Maeztu) from MINECO. C.G. also acknowledges Grant BES-2015-074210 from MINECO.

References

[1] J. Dechargé and D. Gogny, *Phys. Rev. C* **21** (1980) 1568.
[2] CEA web page www-phynu.cea.fr.
[3] J.F. Berger, M. Girod and D. Gogny, *Comp. Phys. Commun.* **63** (1991) 305.
[4] N. Pillet and S. Hilaire, *Eur. Phys. J. A* **53** (2017) 193.
[5] F. Chappert, M. Girod and S. Hilaire, *Phys. Lett. B* **688** (2008) 420.
[6] S. Goriely, S. Hilaire, M. Girod and S. Péru, *Phys. Rev. Lett.* **102** (2009) 242501.
[7] B. Friedman and V. Pandharipande, *Nuc. Phys. A* **361** (1981) 502.
[8] D.T. Loan, H.H. Tan, D.T. Khoa and J. Margueron, *Phys. Rev. C* **83** (2011) 065809.
[9] R. Sellahewa and A. Rios, *Phys. Rev. C* **90** (2014) 054327.
[10] C. Gonzalez-Boquera, M. Centelles, X. Viñas and A. Rios, *Phys. Rev. C* **96** (2017) 065806
[11] C. Gonzalez-Boquera, M. Centelles, X. Viñas and L.M. Robledo, *Phys. Lett. B* **779** (2018) 195.

[12] P.B. Demorest, T. Pennucci, S.N. Ransom, M.S.E. Roberts and J.W.T. Hessels, *Nature* **467** (2010) 1081.
[13] J. Antoniadis et al., *Science* **340** (2013) 6131.
[14] E. Chabanat, P. Bonche, P. Haensel, J. Meyer and R. Schaeffer, *Nuc. Phys. A* **635** (1998) 441.
[15] M. Centelles, X. Roca-Maza, X. Viñas and M. Warda, *Phys. Rev. Lett.* **102** (2009) 122502.
[16] X. Viñas, M. Centelles, X. Roca-Maza and M. Warda, *Eur. Phys. J. A* **50** (2014) 27.
[17] W.D. Myers and W. Swiatecki, *Ann. Phys.* **55** (1969) 395.
[18] P. Danielewicz and J. Lee, *Nuc. Phys. A* **922** (2014) 1.
[19] F. Chappert, Ph.D. thesis, Université Paris-Sud XI, 2007, https://tel.archives-ouvertes.fr/tel-00177379/en/.
[20] F. Chappert, N. Pillet, M. Girod, J.-F. Berger, *Phys. Rev. C* **91** (2015) 034312.
[21] X. Roca-Maza et al., *Phys. Rev. C* **87** (2013) 034301.
[22] B.K. Agrawal, S. Shlomo and V.K. Au, *Phys. Rev. C* **72** (2005) 014310.
[23] J. Piekarewicz, *Phys. Rev. C* **83** (2011) 034319.
[24] F.J. Fattoyev and J. Piekarewicz, *Phys. Rev. Lett.* **111** (2013) 162501.
[25] L.M. Robledo, HFBaxial computer code 2002.
[26] L.M. Robledo and G.F. Bertsch, *Phys. Rev. C* **84** (2011) 054302.
[27] G. Audi, M. Wangh, A. Waspra, F. Kondev, M. MacCormick, X. Xu and B. Pfeiffer, *Chin. Phys. C* **36** (2012) 1287.